Available online at www.sciencedirect.com
ScienceDirect
Developmental Biology 312 (2007) 572–581
DEVELOPMENTAL BIOLOGY
www.elsevier.com/developmentalbiology

Trps1 regulates proliferation and apoptosis of chondrocytes through Stat3 signaling

Hiroki Suemoto [a], Yasuteru Muragaki [a,*], Katsuhiro Nishioka [a], Misako Sato [a,1], Akira Ooshima [a,1], Shunji Itoh [a], Ikuji Hatamura [a], Michitaka Ozaki [b], Attila Braun [c], Erika Gustafsson [c], Reinhard Fässler [c]

[a] *Department of Pathology I, Wakayama Medical University, 811-1 Kimiidera, Wakayama 641-0011, Japan*
[b] *Department of Surgery I, Hokkaido University Graduate School of Medicine, Hokkaido, Japan*
[c] *Department of Molecular Medicine, Max Planck Institute of Biochemistry, 82152 Martinsried, Germany*

Received for publication 21 July 2007; revised 14 September 2007; accepted 1 October 2007
Available online 10 October 2007

Abstract

Mutations in the *TRPS1* gene lead to the tricho-rhino-phalangeal syndrome, which is characterized by skeletal defects and abnormal hair development. The *TRPS1* gene encodes an atypical member of the GATA-type family of transcription factors. Here we show that mice with a disrupted *Trps1* gene develop a chondrodysplasia characterized by diminished chondrocyte proliferation and decreased apoptosis in growth plates. Our analyses revealed that Trps1 is a repressor of Stat3 expression, which in turn controls chondrocyte proliferation and survival by regulating the expression of cyclin D1 and Bcl2. Our conclusion is supported (i) by siRNA-mediated depletion of Stat3 in Trps1-deficient chondrocytes, which normalized the expression of cyclin D1 and Bcl2, (ii) by overexpression of Trps1 in ATDC5 chondrocytes, which diminished Stat3 levels and increased proliferation and apoptosis, and (iii) by mutational analysis of the GATA-binding sites in the *Stat3* gene, which revealed that their integrity is critical for the direct association with Trps1 and for Trps1-mediated repression of Stat3. Altogether our findings identify Trps1 as a novel regulator of chondrocytes proliferation and survival through the control of Stat3 expression.

Keywords: Trps1; Stat3; Chondrocytes; Growth plate; Apoptosis; Proliferation

Introduction

Tricho-rhino-phalangeal syndrome type I and type III (TRPS I or TRPS III) is an autosomal dominant skeletal disorder characterized by short stature and craniofacial anomalies such as a bulbous tip of the nose, a flat and long philtrum, protruding ears and sparse scalp hair (Giedion et al., 1973; Niikawa and Kamei, 1986). TRPS III is more severe than TRPS I and in addition shows brachydactyly (Itin et al., 1996; Nagai et al., 1994). The cause for TRPS I and IIII are mutations in the *TRPS1* gene, which encodes a transcription factor composed of 9 zinc-finger domains, including a single GATA-type DNA binding domain flanked by two potential nuclear localization signals (NLS), and two C-terminal zinc fingers closely related to a domain found in the Ikaros family of lymphoid transcription factors (Momeni et al., 2000). Genotype analysis of patients affected with TRPS identified premature stop mutations in the N-terminal half of TRPS1 leading to truncated proteins, mutations in the GATA binding domain, and in the NLS preventing translocation of TRPS1 into the nucleus (Kaiser et al., 2003b; Ludecke et al., 2001; Momeni et al., 2000). In line with the affected organs of patients TRPS1 is highly expressed in cartilage, developing joints, hair follicles and in the nasal region (Abu et al., 1997; Malik et al., 2001; Kunath et al., 2002). Further support for TRPS1 as disease causing gene comes from gene deletion studies in mice. Mice heterozygous for a deletion of GATA domain in the *Trps1* gene develop thoracic kyphoscoliosis and have structural deficits in cortical and trabecular bones (Malik et al., 2002). Homozygous mice lack vibrissae, have reduced hair follicles and die perinatally due to

* Corresponding author. Fax: +81 73 446 3781.
E-mail address: ymuragak@wakayama-med.ac.jp (Y. Muragaki).
[1] Current address: National Cancer Institute, Bethesda, MD, USA.

0012-1606/$ - see front matter © 2007 Elsevier Inc. All rights reserved.
doi:10.1016/j.ydbio.2007.10.001

respiratory distress caused by abnormalities of the thoracic spine and ribs (Malik et al., 2002). The molecular defects leading to the abnormalities both in human patients and in mice are not known.

TRPS1 is exclusively found in the nucleus and behaves as a potent, sequence-specific transcriptional repressor *in vitro* and *in vivo*. It has been shown that the repressive activity depends on the C-terminal region related to repressive domains found in Ikaros proteins (Malik et al., 2001). Yeast 2-hybrid assays demonstrated that TRPS1 can interact with the light chain 8 protein (LC8a) (Kaiser et al., 2003b) and the ring finger protein RNF4 (Kaiser et al., 2003a). LC8a is usually involved in cytoplasmic transport processes but was shown to co-localize with TRPS1 in distinct, ill-defined structures of the cell nucleus. RNF4 is a transcriptional co-regulator of several genes and is found to be distributed diffusely throughout the cytoplasm and in numerous small granules within the nucleus. DNA binding assays and reporter studies revealed that binding of TRPS1 with either LC8a or RNF4 diminishes the interaction of TRPS1 to GATA consensus sequences and as a consequence releases the repressor activity of TRPS1.

Prior to the implication of TRPS1 in the etiology of TRPS, Chang et al. (1997) isolated the protein from androgen-dependent prostate carcinoma cells and termed it GC79. Their studies proposed that GC79/TRPS1 is repressed by androgens and is involved in apoptosis of prostate cells (Chang et al., 1997, 2002). *In vivo* depletion of androgens by castration leads to increased expression of TRPS1 in the prostate and concomitantly to apoptosis of prostate cells and regression of the organ (Chang et al., 2002). How androgens repress TRPS1 expression and how TRPS1 induces apoptosis of prostate cells is unclear.

To gain mechanistic insights into TRPS1 function we generated mice carrying a null mutation in the *Trps1* gene and found that their growth plate chondrocytes display impaired proliferation and decreased apoptosis caused by increased expression and activation of Stat3.

Materials and methods

Generation of Trps1-null mice

The mouse *Trps1* gene was cloned from a 129/Sv genomic library (UK HGMP Resource Center, Hinxton, UK). The targeting vector consisted of 2.5 kb of 5′ homology followed by an internal ribosomal entry site (IRES)-β-galactosidase gene, the neomycin resistance gene and 8.5 kb of 3′ homology. The targeting vector was linearized and electroporated into R1 embryonic stem (ES) cells (Fassler and Meyer, 1995). Homologous recombination was analyzed by Southern blot using *Bam*HI-digested genomic DNA extracted from ES cell clones. Homologous recombinant clones showed a band of 11 kb in addition to the 15-kb wild-type band. Targeted ES cells were injected into C57BL/6 blastocysts and transferred into uteri of BDF1 pseudopregnant females. Chimeric males were mated with C57BL/6 females.

Production of Trps1-specific antibody

A 1002-bp-long cDNA, coding for 333 amino acid residues of the carboxyl end of Trps1, was cloned in the His-tag containing pQE31 (QIAGEN). The bacterially expressed protein was affinity purified using a nickel column and used to immunize rabbits. Immunization was repeated three times in 2-week intervals.

Histology, immunostaining and in situ hybridization

Whole skeletons of newborn mice were stained with Alcian blue and Alizarin red as described previously (Aszodi et al., 1998). Limbs were removed from newborn mice, fixed in 4% paraformaldehyde overnight at 4 °C, and embedded in Tissue-Tek (Sakura Finetechnical Co., Ltd.) at −130 °C. Frozen sections were cut 5 μm thick and stained with hematoxylin/eosin (HE). For immunostaining, limbs and bronchi were removed from newborn mice and embedded in OCT compound at −130 °C without prior fixation. Frozen sections were cut 5 μm thick, incubated with antibodies against Trps1, phosphorylated Stat3, washed in PBS, incubated with secondary antibodies, and finally mounted in VECTA SHIELD Mounting Medium (Vector Laboratories, Inc.) with DAPI. LacZ staining was performed both in whole mount and in section as previously described (Sakai et al., 2001).

For in situ hybridization digoxygenin (DIG)-labeled sense and antisense cRNA probes were generated from plasmids containing mouse Col2a1, Col10a1, PTH/PTHrP receptor (Ppr), and Indian hedgehog (Ihh) cDNAs using a digoxygenin labeling kit according to the instructions (La Roche). Cryo-sections were hybridized at 50 °C overnight. After stringent washes, the sections were reacted with an alkaline phosphatase-labeled anti-DIG antibody (La Roche). After rinses with Tris-buffered saline (TBS) solution, the sections were developed with BICP/NTB and subsequently mounted.

Overexpression of Trps1 and Stat3-C in ATDC5 cells

A full-length cDNA encoding Trps1 was subcloned in pcDNA3.1 (+) (Invitrogen). The linearized DNA was electroporated into ATDC5 cells (obtained from RIKEN cell bank) and cultured in D/F12 medium (Gibco BRL) containing 10% FBS, 3×10^{-8} M transferrin, and 10 μg/ml sodium selenite and selected with G418 (Sigma). To differentiate ATDC5 cells into chondrocytes, they were treated for 7 days with 10 μg/ml of insulin. ATDC5 cells transfected with a pcDNA3.1 vector only were served as control. To overexpress Stat3, adenovirus encoding a constitutively activated Stat3 (Stat3-C) was transduced into ATDC5 cells. Cells were harvested 7 days after insulin treatment for differentiation.

Knockdown of Stat3 in Trps1-deficient chondrocytes

Synthesized double-strand siRNA oligonucleotides encoding Stat3 were purchased from Invitrogen. Lipofectamine 2000 (Invitrogen) was used as the transfection reagent together with 200 nmol of siRNA following manufacture's directions. Cells were incubated for 6 h and then cultured with media supplemented with 10% FCS. 96 h after transfection, cells were harvested, lysed and assayed by Western blot analysis. Stealth double-strand siRNA was used as a negative control.

Western blotting

ATDC5 cells or isolated primary chondrocytes, respectively, were lysed on ice in RIPA buffer. Lysates were mixed with reducing sample buffer, boiled, separated by SDS-PAGE and blotted on nitrocellulose membranes (S&S) or PVDF membranes (Millipore). The membranes were blocked with TBS containing 0.1% Tween20 and 5% BSA at room temperature for 1 h and finally incubated with primary antibodies at 4 °C overnight. Subsequently the blots were washed with TBS containing 0.1% Tween20, then treated with horseradish peroxidase-conjugated secondary antibodies at room temperature for 1 h and developed with the ECL detection system (Amersham Bioscience). Antibodies used were specific for cyclin D1 (Medical and Biological Laboratories), Bcl-2 (Santa Cruz Biotechnologies), cleaved caspase-3, Stat3, and phosphorylated Stat3 (Cell Signaling Technology).

Detection of BrdU labeling and apoptotic cells

To identify proliferating cells in tissue sections, pregnant females were injected intraperitoneally with 10 mg/ml BrdU (Sigma) 2 h prior to sacrifice. Sections were prepared as described above and treated with a monoclonal anti-BrdU antibody (Boehinger Mannheim) and Envision (Dako) for secondary

antibody, followed by color development. ATDC5 cells were maintained in D-MEM/F12 medium (GIBCO BRL) supplemented with 5% FBS (MBL), 10 μg/ml transferrin (Sigma) and 3×10^{-8} M sodium selenite (Sigma), replacing culture medium every other day. For determining cell proliferation in ATDC5 cells, Cell Proliferation ELISA system (Amersham) was used according to the manufacturer's recommendation. Apoptotic cells were identified with the TUNEL (terminal deoxynucleotidyl transferase mediated dUTP nick end labeling) method using ApopTag peroxidase and Fluorescein in situ apoptosis detection kits (INTERGEN). To induce apoptosis of cultured ATDC5 cells and primary chondrocytes, 0.3 μg/ml Jo2, an agonistic antibody to Fas, and 1.5 μg/ml cyclohexamide were added into the culture medium 48 h prior to the experiments.

Luciferase assay

A 1216-bp fragment corresponding to nucleotides −1178 to +38 of the murine Stat3 promoter was amplified from mouse genomic DNA and subcloned into the pGL3-Basic luciferase reporter vector (Promega). The fragment was inserted into the *Kpn*I–*Xho*I site upstream of the luciferase gene of the pGL3-Basic vector.

Transfections of 0.5×10^5 chondrocytes were carried out with varying amounts of the reporter construct using LipofectAMINE (Invitrogen) according to the manufacture's recommendations. The cells were harvested 24 h after transfection and assayed for both renilla and firefly luciferase activity by using a Dual Lusiferase kit (Promega). Co-transfection of 1 μg of pcDNA-rLUC (renilla luciferase) was used as optimized equalization control. Transfections of the constructs were performed independently and in triplicate.

Site-directed mutagenesis

Site-directed mutagenesis of GATA sites in the Stat3 promoter was performed using QuickChange Site-Directed Mutagenesis Kit (Stratagene) according to the manufacture's recommendations. Briefly, PCR primers encompassing the GATA sites in the Stat3 promoter (−1059 to −1056 and −558 to −555) and flanking sequences were used. The upstream GATA substituted by the GAGA sequence (mutation underlined): 5′-CAAGACGTGAAATAGGTCAGAGAATTTCAAGAGCGTCAAGAC-3′ and 5′-GTCTTGACGCTCTTGAAATTCTCTGACCTATTTCACGTCTTG-3′, and the downstream GATA was substituted with the TAGC sequence (reverse compliment of TATC, mutation underlined): 5′-GAAACAAGTTGGTCAAAACTAGCTTTCAGAATTTCAAGACCC-3′ and 5′-GGGTCTTGAAATTCTGAAAGCTAGTTTTGACCAACTTGTTTC-3′. The PCR was performed with Pfu Turbo polymerase (Stratagene) using the wild-type Stat3 promoter luciferase construct as template. The PCR reaction was digested with *Dpn*I, and the undigested plasmids were transformed into One-shot TOP 10 bacteria. Individual plasmid preparations were sequenced to verify the mutations of the GATA sites.

Chromatin immunoprecipitation (ChIP)

ChIP was performed as described by (Ogasawara et al., 2004). Briefly, chondrocytes were prepared from E18.5 wild-type and mutant epiphyseal cartilage. The cells were fixed with 1% formaldehyde in DMEM at 37 °C for 15 min and then washed with PBS. The cells were resuspended and incubated on ice for 10 min in 2 ml of lysis buffer containing 1% SDS, 10 mM EDTA, 50 mM Tris–HCl, pH8.1, 1 mM PMSF, and 1 μg/ml of aprotinin. The cell lysates were sonicated on ice to fragment the chromosomal DNA. After centrifugation, the supernatants were diluted with dilution buffer containing 0.01% SDS, 1.1% TritonX-100, 1.2 mM EDTA, 16.7 mM Tris–HCl, pH 8.1, 167 mM NaCl, 1 mM PMSF, and 1 μg/ml of aprotinin and were pretreated with a 50% protein G–sepharose at 4 °C for 4 h to avoid a non-specific binding of chromatin to the protein G–sepharose. After a brief centrifugation, the supernatants were incubated with an anti-Trps1 antibody or a control IgG at 4 °C overnight. A 50% protein G–sepharose was then added to the supernatant to allow binding of immunocomplexes to bind protein G–sepharose at 4 °C for 4 h. After washing with low-salt (20 mM Tris–HCl, pH 8.1, 150 mM NaCl, 2 mM EDTA, 0.1% SDS, 1% Triton X-100), high-salt (20 mM Tris–HCl, pH 8.1, 500 mM NaCl, 2 mM EDTA, 0.1% SDS, 1% Triton X-100), LiCl (0.25 M LiCl, 10 mM Tris–HCl, pH 8.1, 1 mM EDTA, 1% sodium deoxycholate, 1% NP40), and TE (10 mM Tris–HCl, pH 8.0, 1 mM EDTA, pH 8.0) wash buffer in sequential order, the protein G-bound immunocomplexes were resuspended in 250 μl of elution buffer (1% SDS, 0.1 M $NaHCO_3$) and the eluates were heated at 65 °C for 6 h to reverse cross-linking. To remove proteins bound to DNA, the eluates were treated with proteinase K and the DNA was precipitated with ethanol after purification with phenol–chloroform. The Stat3 promoter sequence was amplified by 35 PCR cycles with the following primers: 5′-CTGTACTCCCAACATACAAGACGTG-3′ and 5′-GCTAACACACACAGAGAGAAAGCCC-3′ (positions −1094 to −846), and 5′-AGACCCCAGAGTGGAGTTACAAATG-3′ and 5′-CTGACACGAATACACAGTACTTGGC-3′ (positions −718 to −465) (Shi et al., 1996).

Results

Trps1-null mice die from respiratory failure and suffer from chondrodysplasia

To inactivate the *Trps1* gene part of exon 3 and intron 3 was replaced by an IRES-β-galactosidase and neomycin cassettes (Fig. 1A). Two independently targeted ES cell clones were used to generate heterozygous ($Trps1^{+/-}$) mice, which were fertile and had no apparent phenotype except that they frequently developed scarce fur on their back at the age of 6–8 months (data not shown). Homozygous ($Trps1^{-/-}$) mice were born at the expected Mendelian distribution (Fig. 1B). Immunohistochemistry of limb sections with Trps1-specific polyclonal antisera confirmed that mutant mice lack Trps1 expression. While wild-type joint surfaces showed strong expression, Trps1 signals were absent from digits of $Trps1^{-/-}$ mice (Fig. 1C). LacZ staining overlapped with the antibody staining in digits of heterozygous mice indicating that the β-galactosidase gene is faithfully controlled by the Trps1 promoter (Fig. 1D).

Homozygous mice were dwarfed and began labored respiration after birth, became cyanotic and finally died of respiratory distress. Lungs derived from homozygous mutant mice were smaller than those of wild type and showed reduced air space with thickened septae in light microscopy. The trachea from homozygous Trps1-deficient mice was normally sized but contained abnormal cartilage plates consisting of small chondrocyte nests instead of a fused cartilage ring (Supplementary Fig. 1). The small cartilage nodules led to a collapse of the bronchial lumen with severe narrowing of the air space.

$Trps1^{-/-}$ mice showed severe hair follicle abnormalities and growth retardation. To determine the reason(s) for the growth retardation, we performed whole-mount skeletal staining with Alizarin red for bones and Alcian blue for cartilage (Fig. 1E). $Trps1^{-/-}$ mice had shortened maxillary and mandibular bones, shortened long bones in limbs, and a short, thin and bifurcated sternum with an abnormally widened rib cage. The long bones in mutant mice were 85±3% shorter than those in the wild-type littermates (Fig. 1F). The calcification of the sternum was reduced, as was the formation of the primary ossification centres in developing long bones (Fig. 1F and Supplementary Fig. 2). Approximately 30% of mutant mice had an extra rib, which was unilaterally attached to the sternum. The mutant rib cartilage was fragile and easy to break during preparation. This fragility might cause and/or

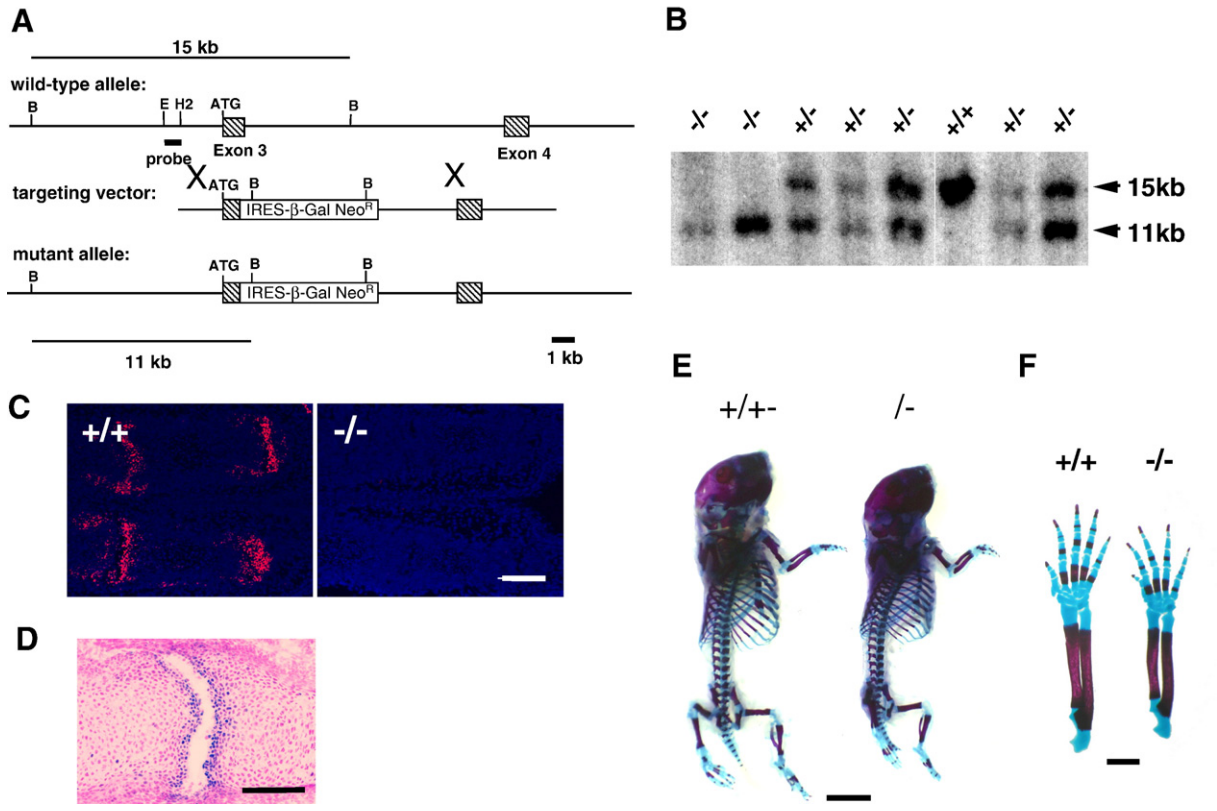

Fig. 1. Targeted disruption of mouse Trps1. (A) Structure of wild-type allele, targeting construct, and mutant allele after homologous recombination. Boxes indicate exons. The location of the fragment used as a probe for Southern blot is shown, as well as the expected sizes of the two *Bam*HI fragments detected for wild-type and mutant alleles. (B) Southern blot analysis of tail genomic DNA isolated from the progeny of a heterozygous cross. Fragments corresponding to wild-type (15 kb) and mutant (11 kb) alleles are shown. +/+, wild-type; +/−, heterozygous; −/−, homozygous. (C) Immunofluorescent staining of newborn digits with an anti-Trps1-specific antibody (red) confirms complete deletion of the Trps1 protein in the mutant mouse (right). Arrows indicate the location of the joints. Nuclei are stained with DAPI. Scale bar: 50 μm. (D) LacZ staining shows that Trps1-driven β-galactosidase is expressed in the interphalangeal joint. Scale bar: 100 μm. (E) Whole-mount skeletal staining of newborn wild-type (+/+) and mutant (−/−) mice with Alizarin red S and Alcian blue. Scale bar: 5 mm. (F) Alizarin red S and Alcian blue staining of forelimb in newborn wild-type (+/+) and mutant (−/−) mice. Scale bar: 1 mm.

contribute to the deformity of the rib cage and the abnormal bronchial rings.

Differentiation of Trps1−/− chondrocytes seems normal

Longitudinal growth of bones is controlled by endochondral ossification, which occurs in growth plates. Immunohistochemistry revealed that Trps1 was present in the articular, proliferative and prehypertrophic chondrocytes (Fig. 2A) suggesting that Trps1 exerts an autonomous function in growth plates.

Alizarin red/Alcian blue staining of the Trps1$^{-/-}$ tibia revealed a narrow epiphyseal cartilage, which was, however, longer than in the wild-type tibia (Fig. 2B). Histological sections showed an extended length of proliferative zone in Trps1$^{-/-}$ growth plates (Fig. 2C) with a reduced chondrocyte density (see blow up of Fig. 2C). The cell densities per 10 mm^2 were reduced by 30% in the proliferative zone in Trps1$^{-/-}$ growth plates when compared with growth plates from control littermates (Fig. 2D). These findings indicate that Trps1 controls chondrocyte number and, similarly like in the tracheal rings, the morphology of the growth plate.

To determine whether differentiation of Trps1$^{-/-}$ is altered we performed in situ hybridization analyses with several differentiation markers. Neither Col2a1 nor Col10a1 mRNA expression differed between wild-type and Trps1$^{-/-}$ growth plates (Fig. 2E). The expression of Indian hedgehog (Ihh) and parathyroid hormone/parathyroid hormone-related peptide receptor (Ppr) was also similar between wild-type and Trps1$^{-/-}$ growth plates.

Trps1 regulates proliferation of chondrocytes

To test whether the reduced chondrocyte numbers in Trps1$^{-/-}$ growth plates were caused by a proliferation defect we measured BrdU incorporation in the epiphyseal cartilage. The BrdU labeling index was significantly decreased in Trps1$^{-/-}$ growth plates (Figs. 3A, B). This was further confirmed by Western assays, which revealed a strong reduction in cyclin D1 expression in freshly isolated Trps1$^{-/-}$ chondrocytes (Fig. 3C). The amount of cyclin D1 was reduced by 40% and 20% in Trps1$^{-/-}$ chondrocyte extracts from epiphyseal and rib cartilage, respectively. Immunohistochemistry of proliferative chondrocytes with an anti-cyclin D1 antibody also

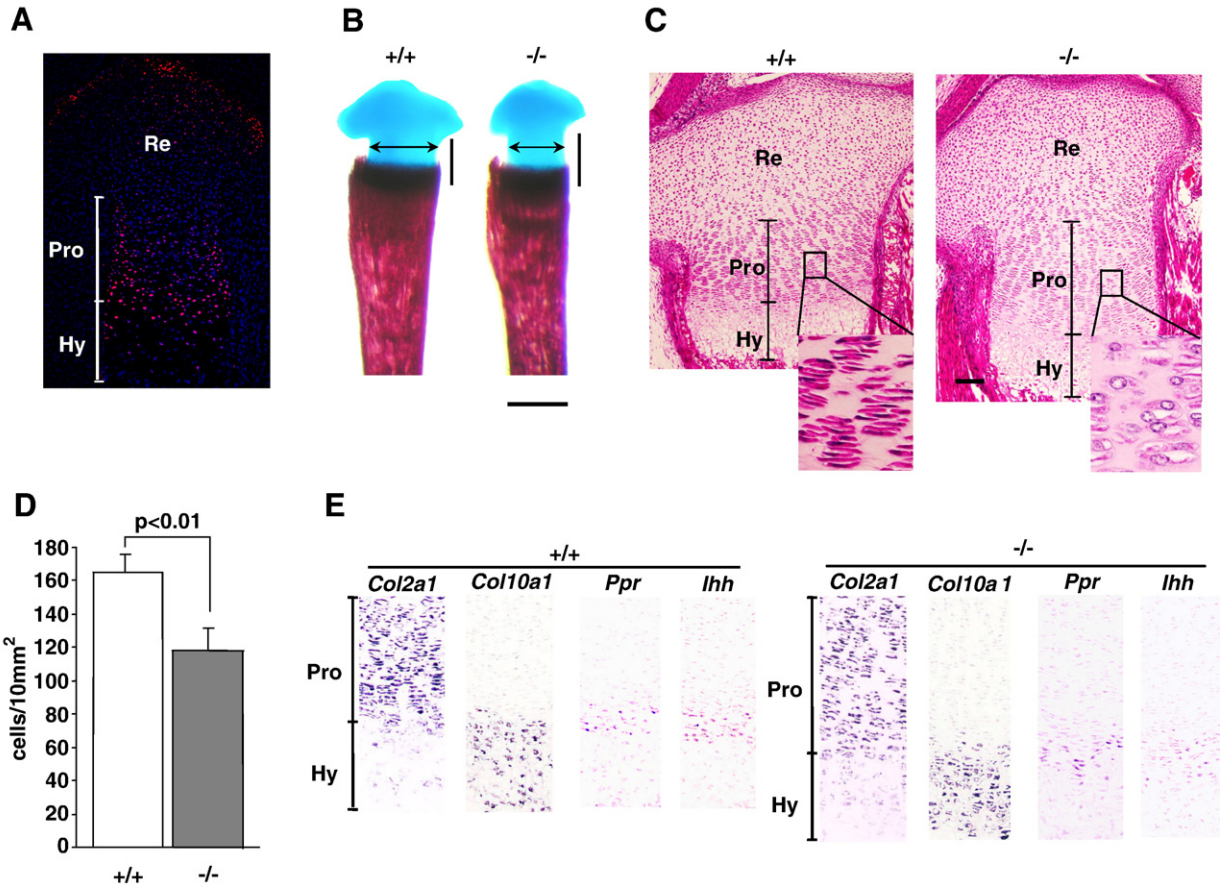

Fig. 2. Chondrocyte differentiation and function in the tibial epiphyseal cartilage. (A) Immunohistochemical localization of Trps1 in the growth plate. The highest intensity of immunoreaction (red or pink) is seen in the articular and prehypertrophic chondrocytes. Nuclei were stained with DAPI (blue). The length of each zone is indicated by a line. Re: resting chondrocytes, Pro: proliferating zone, Hy: hypertrophic zone. (B) Alizarin red/Alcian blue staining of the tibia. Bi-directional arrows and vertical bars represent the width and the length of the growth plates, respectively. Scale bar: 0.5 mm. (C) All sections are stained with hematoxylin and eosin. The length of the epiphyseal cartilage is longer in Trps1$^{-/-}$ growth plates, the proliferating (Pro) zone is extended. Boxed areas are shown a blow ups. Scale bar: 100 μm. (D) The comparison of cell density in the proliferating zone. The white and black columns show the number of chondrocytes per 10 mm^2 in the proliferating zone of wild-type (+/+) and Trps1-deficient (−/−) mice, respectively. Five arbitrary areas were selected from the proliferative zone and the number of chondrocytes was counted. (E) Histological analysis of chondrocyte differentiation by in situ hybridization. The sections from newborn tibia were hybridized with probes specific for Col2a1, Indian hedgehog (Ihh), Pth/Pthrp receptor (PPR), and Col X, markers for the proliferating, prehypertrophic, and hypertrophic chondrocytes. Each zone of chondrocytes is positive for the zone-specific marker.

demonstrated that the positively stained cells are much less in Trps1$^{-/-}$ proliferative chondrocytes as compared to wild-type counterparts (Fig. 3D).

Next we investigated whether overexpression of Trps1 is enhancing chondrocyte proliferation. To this end we transfected a Trps1 expression construct into the ATDC5 chondrocyte cell line. Whereas mock-transfected cells expressed low levels of Trps1, transfection of the Trps1 expression vector increased Trps1 levels by 4-fold (Fig. 3D). Cells overexpressing Trps1 exhibited a significantly increased BrdU incorporation (Fig. 3E) further indicating that Trps1 promotes chondrocyte proliferation.

Trps1 regulates apoptosis of hypertrophic chondrocytes

Despite the reduced cell proliferation, we observed a normal sized zone of hypertrophy in growth plates of newborn Trps1$^{-/-}$ mice (Fig. 2C), raising the question whether chondrocytes were also protected from apoptosis. Trps1 was shown to execute androgen-dependent apoptosis (Chang et al., 2000, 2002) and terminally differentiated, hypertrophic chondrocytes are eliminated by triggering apoptosis (Hatori et al., 1995).

The number of TUNEL-positive hypertrophic chondrocytes was dramatically reduced in mutant growth plates, while TUNEL-positive cells were clearly detectable in wild-type hypertrophic zone (Fig. 4A). Antibody staining for cleaved caspase-3 also revealed a reduced number of positively stained cells in mutant growth plates when compared to controls (data not shown). Western blot analyses further confirmed the reduced expression of cleaved caspase-3 in chondrocyte lysates derived from Trps1$^{-/-}$ rib and epiphyseal cartilage (Fig. 5A). In addition, we found that the expression of Bcl-2 was increased by at least two-fold in Trps1$^{-/-}$ growth plate chondrocytes (Fig. 5A), while expression of the anti-apoptotic proteins Bcl-X_L and FLIP was normal (data not shown).

To test the functional significance of the reduced activity of caspase-3 and increased expression of the anti-apoptotic protein Bcl-2, we induced apoptosis in cultured primary chondrocytes

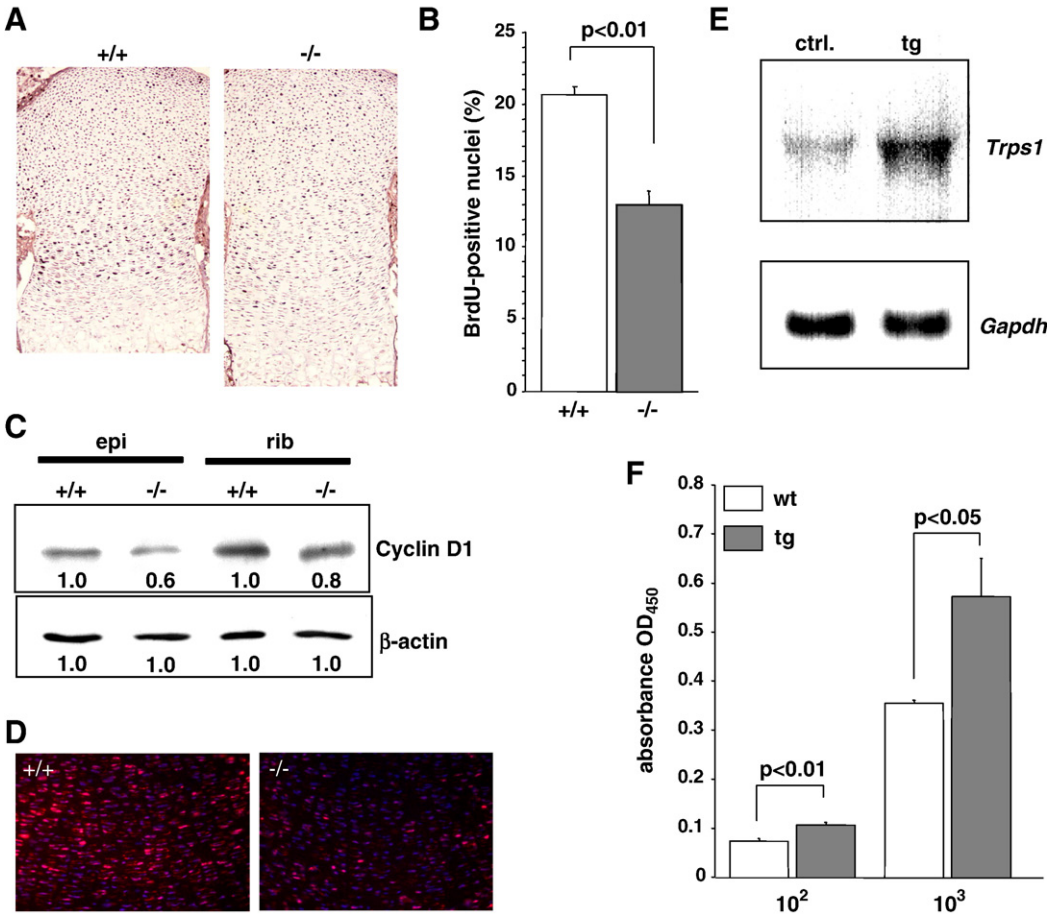

Fig. 3. Chondrocyte proliferation is regulated by Trps1. (A) Consecutive sections of newborn knee joints were stained with an anti-BrdU antibody. (B) The numbers of BrdU-positive and -negative chondrocytes were counted. The ratio of positive to total chondrocytes is significantly decreased in Trps1$^{-/-}$ epiphyses as compared to wild-type counterparts ($p<0.01$). (C) Western blot analysis of cyclin D1 with extracted protein from epiphyseal cartilage (epi) and rib cartilage (rib) of wild-type (+/+) and mutant (−/−) mice. Numbers represent relative intensity to that of wild-type. (D) Immunohistochemistry of cyclin D1 in proliferative zone of wild-type (+/+) and mutant (−/−) growth plate. The immunoreaction (red) is seen in the proliferative chondrocytes. Nuclei were stained with DAPI (blue). (E) Northern blot analysis showing that ATDC5 cells transfected with a CMV promoter-driven Trps1 cDNA construct (tg) express a higher amount of Trps1 mRNA. ctrl: ATDC5 cells transfected with a CMV promoter vector only. (F) BrdU incorporation as determined by cell proliferation of ATDC5 cells with a vector only (wt) and a CMV promoter-driven Trps1 cDNA construct (tg). ATDC5 cells with the initial cell number of 10^2 and 10^3 were used for the assay. Results represent means ± standard deviation of four samples.

by treating them with the Fas cross-linking antibody Jo2. Subsequent TUNEL assays showed that Trps1$^{-/-}$ chondrocytes were significantly less prone to apoptosis than wild-type chondrocytes (Fig. 4B). In line with these findings, Trps1-overexpressing ATDC5 chondrocyte cells treated with Jo2 antibodies exhibited a significantly increased apoptosis rate (Fig. 4C) and decreased levels of Bcl-2 (Fig. 5C) when compared to mock-transfected cells. These data suggest that Trps1 can regulates chondrocytes proliferation and promote their apoptosis by modulating Bcl-2 levels.

Trps1 regulates proliferation and apoptosis through Stat3

Proliferation of growth plate chondrocytes is regulated by various external signals such as growth factors, hormones and cytokines (for a review, see Karsenty and Wagner, 2002). To test whether their expression is altered we performed a series of in situ hybridization of E15.5 tibial sections and found that the expression of Fgf receptors 1, 2 and 3, Fgf 9, Fgf 18, Bmp 2 and Bmp 4 were indistinguishable between wild-type and mutant tissues (data not shown).

Recent findings demonstrated that overexpression of Stat3 in liver is sufficient to increase Bcl-2 and support hepatocyte survival (Haga et al., 2003). Since Trps1$^{-/-}$ chondrocytes were less prone to apoptosis (Fig. 4A) and their Bcl-2 levels were increased (Fig. 5A), we examined the expression of Stat3 in mutant chondrocytes. Interestingly, Trps1$^{-/-}$ chondrocytes had increased levels of total and phosphorylated Stat3 when compared with wild-type chondrocytes (Fig. 5A). Immunohistochemistry revealed an elevated number of chondrocytes with nuclear phospho-Stat3 in Trps1$^{-/-}$ growth plates (Fig. 5B), while the expression of other Stats including Stat1 and Stat5 were not changed (data not shown). Since overexpression of Trps1 in ATDC5 chondrocytes decreased the levels and activity of Stat3 (Fig. 5C) we conclude that Trps1 may act as a transcriptional repressor of the *Stat3* gene in chondrocytes.

To test whether Stat3 acts downstream of Trps1 in chondrocytes we depleted Sat3 expression using specific siRNA.

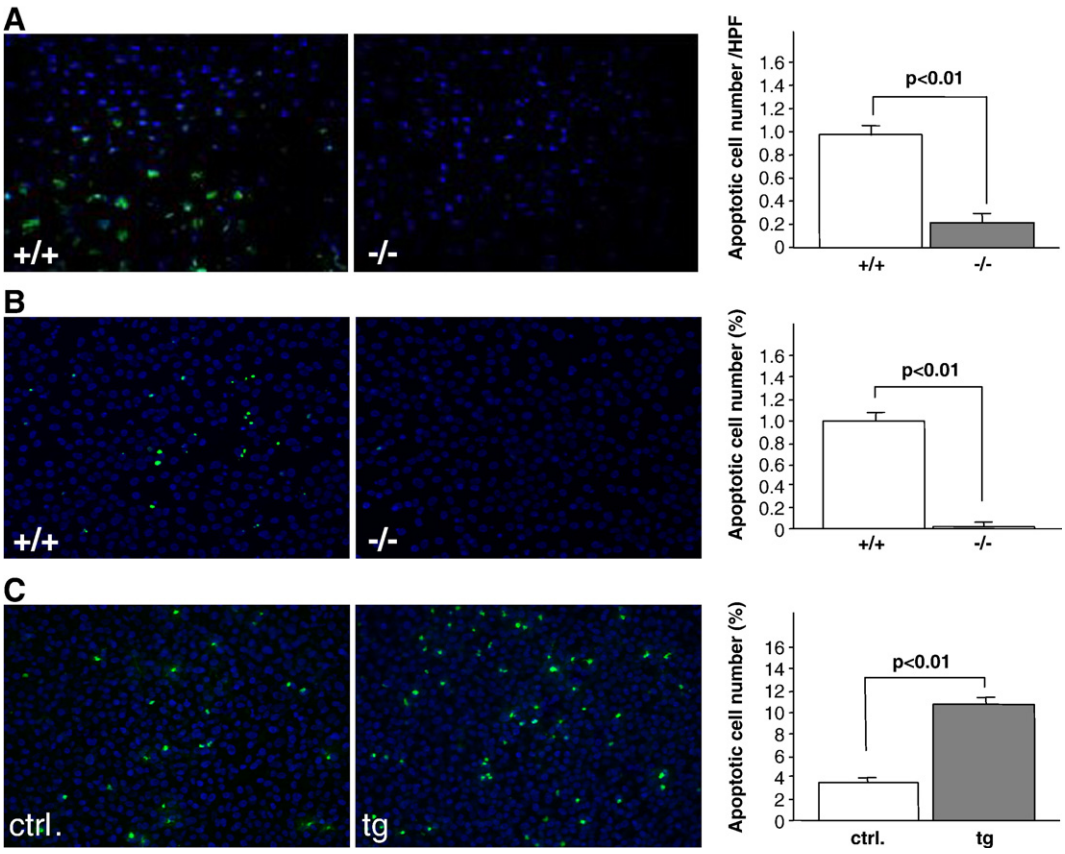

Fig. 4. Trps1 regulates apoptosis of chondrocytes. (A) TUNEL staining for the hypertrophic chondrocytes of the growth plate from newborn wild-type (+/+) and mutant (−/−) mice. The number of TUNEL-positive cells is less in mutant mice (−/−) as compared to wild-type mice (+/+) ($p<0.01$). DAPI (blue) was used for nuclear staining. (B) TUNEL staining of primary chondrocyte cell culture from wild-type (+/+) and mutant (−/−) mice. Apoptosis was induced by treatment with Jo2 antibodies. The ratio of TUNEL-positive cells to the total cells is increased in mutant (−/−) chondrocytes as compared to wild-type (−/−) counterparts ($p<0.01$). (C) TUNEL staining of ATDC5 cells with a vector only (ctrl) and a CMV promoter-Trps1 cDNA construct (tg). Note that the ratio of TUNEL-positive cells is clearly increased upon overexpression as compared to control ($p<0.01$).

The Stat3-specific siRNA led to an almost complete depletion of the Stat3 protein, while control siRNAs neither affected Stat3 levels nor phosphorylation (Fig. 5D). Interestingly, depletion of Stat3 reversed the Trps1$^{-/-}$ phenotype and increased cyclin D1 and decreased Bcl-2 levels (Fig. 5D).

To further confirm the function of Stat3 on proliferation and apoptosis in chondrocytes we overexpressed a constitutively activated form of Stat3 (Stat3-CA) in ATDC5 cells. This led to 3-fold elevation of Bcl-2 and a 50% decrease in cyclin D1 expression (Fig. 5E). Moreover, Stat3-CA expressing ATDC5 cells displayed a significantly reduced proliferation rate (Fig. 5F). Together these data indicate that Trps1 regulates proliferation and apoptosis of chondrocytes by suppressing Stat3 signaling.

Trps1 regulates the expression of Stat3 gene via GATA sites in the promoter region

The upregulation of Stat3 in Trps1$^{-/-}$ chondrocytes suggests that Trps1 is suppressing transcription of the *Stat3* gene by directly binding to the *Stat3* promoter region. The *Stat3* promoter region contains two putative GATA sequences (Shi et al., 1996) and therefore we next investigated whether one or both of them are responsible for the suppression of *Stat3* transcription. We constructed luciferase reporter constructs, in which the *Stat3* promoter region harbored mutations in either one or both GATA sequences and expressed them in control and Trps1$^{-/-}$ chondrocytes. As shown in Fig. 6A, luciferase activity was significantly reduced in wild-type compared to Trps1$^{-/-}$ chondrocytes. Ablation of either GATA site increased luciferase activity 3-fold in wild-type chondrocytes (Fig. 6A) indicating that both GATA sites are essential to suppress *Stat3* transcription.

Next we performed chromatin immunoprecipitation (ChIP) to show that Trps1 binds to the GATA sites in the *Stat3* promoter. The assay revealed that we could immunoprecipitate the GATA sites with anti-Trps1 antibodies in wild-type chondrocytes (Fig. 6B), while neither immunoprecipitation with control IgGs nor genomic DNA from Trps1$^{-/-}$ chondrocytes produced the expected PCR product (Fig. 6B).

Discussion

Mutations in the *TRPS1* gene cause tricho-rhino-phalangeal syndromes, which are characterized by hair, craniofacial and skeletal abnormalities (Momeni et al., 2000). TRPS1 is a

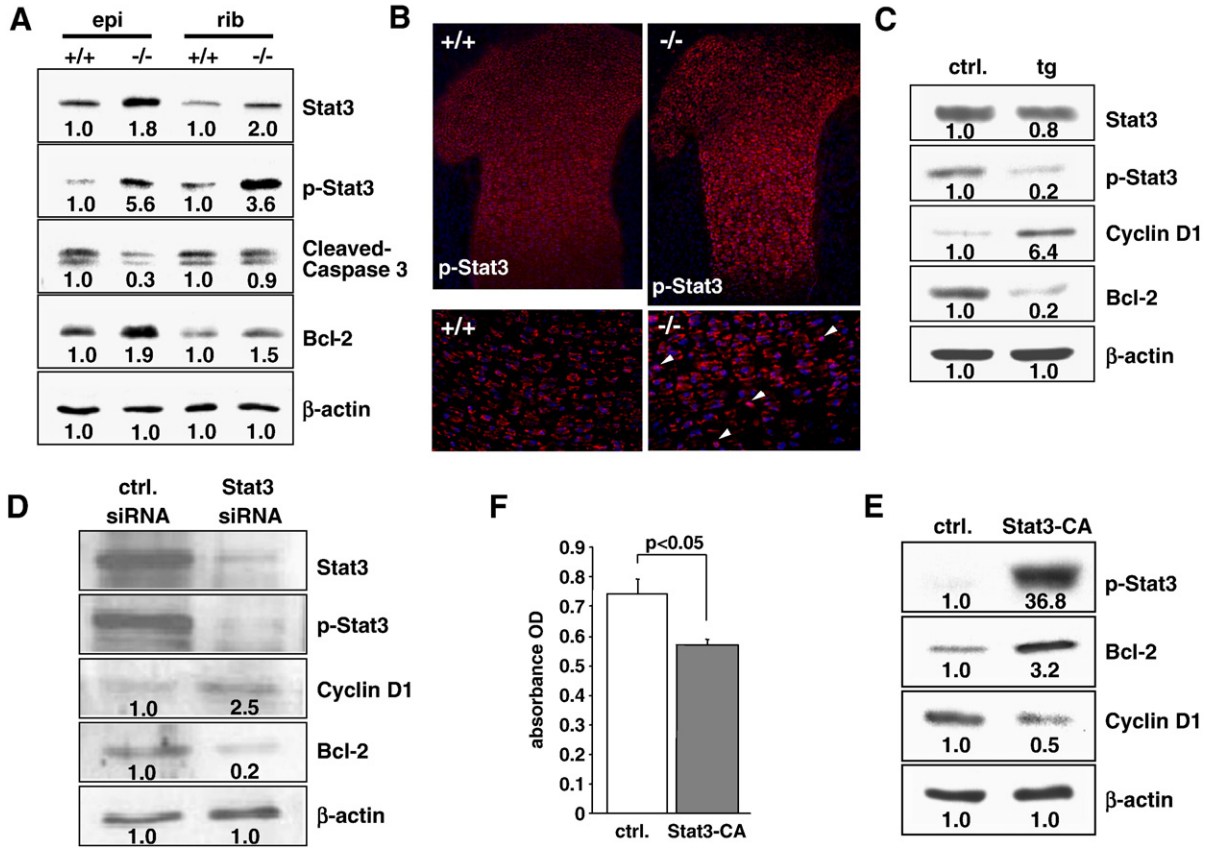

Fig. 5. Ablation of Trps1 leads to an increased levels of Stat3 and phosphorylated Stat3. (A) Western blot analyses of Stat3, phosphorylated Stat3, cleaved caspase-3, and Bcl-2 with cell extracts of primary chondrocytes from epiphyses (epi) and rib cartilage (rib) of wild-type (+/+) and mutant (−/−) mice. Number represents relative intensity to that of wild type. (B) The localization of phosphorylated Stat3 in epiphyseal cartilage from wild-type (+/+) and mutant (−/−) mice (top). Translocation of phosphorylated Stat3 (red) in growth plate chondrocytes from wild-type (+/+) and mutant (−/−) mice (bottom). Nuclei were stained with DAPI (blue). Note that translocated Stat3 is seen in pink (arrow heads) because red color is superimposed on blue color. (C) Western blot analysis of Stat3, phosphorylated Stat3, cyclin D1, and Bcl-2 with cell extract from control (ctrl) and Trps1 overexpressing (tg) ATDC5 cells. Number represents relative intensity to that of ctrl. (D) Knockdown of Stat3 in mutant chondrocytes using Stat3 siRNAs. Western blots were performed with cell extract of the primary chondrocytes from mutant epiphyseal cartilage. Stealth double-strand siRNA (Invitrogen) was used as a control (ctrl). Number represents relative intensity to that of ctrl. (E) Western blot analysis of phosphorylated Stat3, cyclin D1, and Bcl-2 with cell extracts from ATDC5 cells infected with an adenovirus vector only (ctrl) and one with a constitutively active Stat3 (Stat3-CA), respectively. (F) Cell proliferation assay of ATDC5 cells infected with an adenovirus vector only (ctrl) and one with a constitutively active Stat3 (Stat3-CA).

nuclear protein with a single GATA-type zinc finger, which was shown to bind GATA sequences and repress gene transcription (Malik et al., 2001). To test the functional properties of the GATA-type zinc finger motif Malik et al. (2002) engineered mice, which expressed a GATA-type zinc finger-deficient Trps1 protein ($Trps1^{\Delta gt}$). They found that heterozygous $Trps1^{+/\Delta gt}$ mice are fertile, develop structural deficits in cortical and trabecular bones and display facial abnormalities that resemble TRPS I patients. Homozygous $Trps1^{\Delta gt/\Delta gt}$ mice die perinatally of respiratory failure and have pronounced hair follicle defects. Although this study directly assigns an important role of Trps1 for skeletal and hair follicle development, it did not show how Trps1 regulates skeletal development at the molecular level. In the present paper we generated Trps1-deficient mice to address this question.

We ablated the *Trps1* gene by disrupting the ATG-containing exon 3 and found that heterozygous mice ($Trps1^{+/-}$) have reduced number of hair follicles in their back skin but otherwise develop and age normally. The abnormalities in $Trps1^{+/-}$ mice are restricted to the hair coat of the back and are less pronounced than in $Trps1^{+/\Delta gt}$ mice (Malik et al., 2002). An explanation for the different severity could be that a GATA-deficient Trps1 expressed from the $Trps1^{\Delta gt}$ allele is more efficiently antagonizing the wild-type Trps1 than the short N-terminal, 282 amino acid long polypeptide produced in our $Trps1^{+/-}$ mice.

The $Trps1^{-/-}$ mice die perinatally of respiratory distress likely caused by the absent cartilage plates in bronchi and display pronounced skeletal and hair follicle defects. The skeletal abnormalities range from growth retardation to skeletal and facial abnormalities and closely resemble the abnormalities seen in TRPS patients. The growth retardation was visible at birth, affected the longitudinal growth all long bones and was associated with abnormal growth plate morphology including an extended length and narrowing of mutant growth plates, a significantly reduced number of cells with an abnormal shape in the proliferative zone and a normal number of cells in the hypertrophic zone. We do not know the reason for the increased length of $Trps1^{-/-}$ growth plates despite the severely reduced cellularity in the proliferative zone. A possible explanation

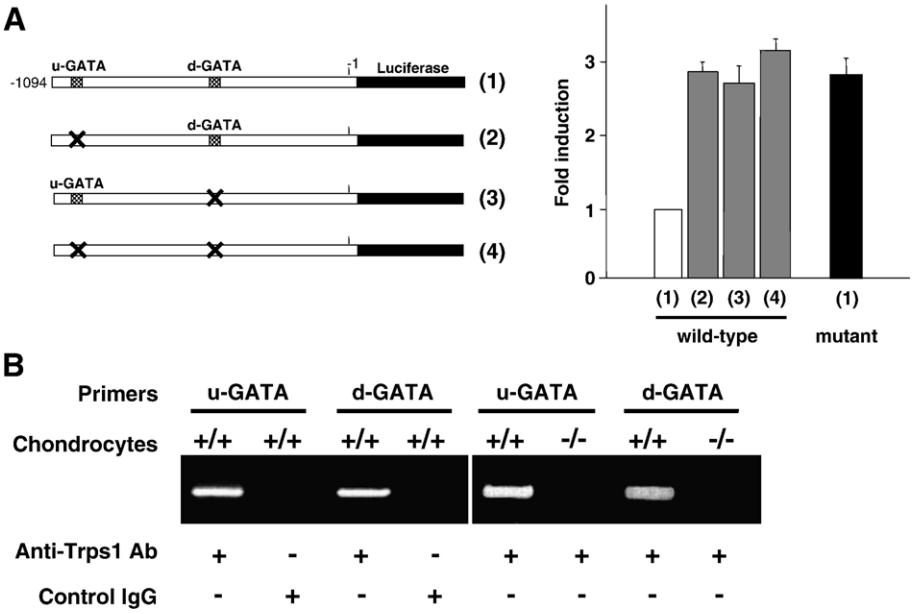

Fig. 6. Transcriptional regulation of Stat3 by Trps1. (A) Mutation analysis of the Stat3 promoter using the luciferase reporter. Transactivation of Stat3 luciferase reporter constructs with either wild-type (1) or mutant (2–4) GATA-binding sites (left panel) in wild-type or mutant chondrocytes. (1) Wild-type Stat3 promoter construct, (2) mutant construct with a mutation in the upstream GATA site, (3) mutant construct with a mutation in the downstream GATA site, (4) mutant construct with a mutation in both the upstream and downstream GATA sites. (B) Chromatin immunoprecipitation (ChIP) assay. PCR amplification of DNA fragments with GATA site is shown. DNA templates were prepared from wild-type (+/+) and mutant (−/−) chondrocytes.

could be that loss of Trps1 function interferes with the expression of cartilage matrix proteins, or integrin-mediated adhesion and/or the organization of the cytoskeleton, which are known to profoundly affect chondrocytes shape and growth plate morphology (Aszodi et al., 2003). Alternatively, the strong expression of Trps1 in the perichondrial chondroblasts may be critically important for appositional chondrogenesis and the widening of growth plates. These possibilities are investigated at the moment.

In search for a mechanistic explanation for the decreased number of proliferating chondrocytes in Trps1$^{-/-}$ growth plates we identified a signaling pathway, in which Trps1 undertakes the principal task to bind both GATA sequences in the Stat3 promoter and then represses Stat3 transcription, which in turn is enhancing cyclin D1 expression. The following evidence supports this notion: first, we observed that Trps1$^{-/-}$ chondrocytes express significantly elevated levels of total and phosphorylated Stat3 and dramatically reduced levels of cyclin D1. Stat3 is known to regulate proliferation with different outcomes depending on the cell type (for a review, see Levy and Lee, 2002). In a pro-B cell line and in several breast and ovarian cancer cells Stat3 was shown to trigger cyclin D1 expression and the G1 to S phase transition (Fukada et al., 1998; Li et al., 2004), while in granulocytes and hepatocytes Stat3 represses cyclin D1 expression and negatively regulates cell proliferation (Lee et al., 2002; Matsui et al., 2002). Second, siRNA-mediated depletion of Stat3 in primary Trps1$^{-/-}$ chondrocytes restores cyclin D1 to normal levels. Conversely, adenoviral overexpression of constitutively activated Stat3 in the chondrogenic ATDC5 cells induces a dramatic downregulation of cyclin D1 expression and diminishes their proliferation rate. Third, the activity of a Stat3 promoter-driven luciferase reporter is repressed in wild-type chondrocytes. The repression is efficiently relieved upon mutation of either of the two or both GATA sequences in the Stat3 promoter. Finally, chromatin immunoprecipitation assays revealed that Trps1 is bound to the upstream as well as downstream GATA sequence.

We also made the surprising observation that despite reduced cellularity in the proliferative zones of Trps1$^{-/-}$ growth plates the number of cells in hypertrophic zones was unaffected. Hypertrophic chondrocytes are eliminated at the chondro-osseous interzone by apoptosis (Shapiro et al., 2005). The signaling pathway leading to apoptosis is not known. In line with an important role of Trps1 in regulating apoptosis of hypertrophic chondrocytes, we observed a significantly reduced number of TUNEL-positive cells in the hypertrophic zone of Trps1$^{-/-}$ mice and observed that primary Trps1$^{-/-}$ chondrocytes are resistant to the apoptosis-inducing action of the agonistic anti-Fas antibody Jo2. The high level and activity of Stat3 in Trps1$^{-/-}$ chondrocytes together with the well documented role of Stat3 as a survival promoting signaling molecule (Levy and Lee, 2002) made Stat3 an obvious candidate for controlling chondrocyte survival downstream of Trps1. This assumption was corroborated with several experiments. Immunostaining of wild-type growth plates revealed that Stat3 signals are gradually disappearing when chondrocytes become hypertrophic and are absent at the chondro-osseous interzone where cells apoptose. In sharp contrast, Trps1$^{-/-}$ growth plate chondrocytes display an intense phosphorylated Stat3 staining, which extends into the hypertrophic zone. Interestingly, Western blot assays revealed that the elevated levels of phosphorylated Stat3 in Trps1$^{-/-}$ chondrocytes are associated with an elevation of Bcl-2 suggesting that Stat3 may act, at least in part, in a Bcl-2-dependent manner (Takeda et al., 1998; Oritani et al., 1999).

This seems clearly to be the case since (i) the elevated Bcl-2 expression is restored to normal levels by siRNA-mediated depletion of Stat3 in Trps1$^{-/-}$ chondrocytes, (ii) overexpression of Stat3 in ATDC5 cells is increasing Bcl-2, and (iii) overexpression of Trps1 in ATDC5 cells leads to a decrease in Bcl-2 expression and apoptosis.

It is possible that also Stat3/Bcl-2-independent mechanisms contribute to increased hypertrophic chondrocyte survival in Trps1$^{-/-}$ growth plates. The absence of Trps1 from the chondro-osseous interzone, however, excludes a potential pro-survival role for Trps1 interacting proteins such as the transcriptional co-activator RNF4 (Kaiser et al., 2003a) or dynein light chain LC8a (Kaiser et al., 2003b), which blocks Bcl-2 activity by binding the Bcl-2 family member Bim (Puthalakath et al., 1999).

Acknowledgments

We thank Dr. Attila Aszodi for teaching primary chondrocytes isolation, lively discussions and careful reading of the manuscript. This work was supported by Grants-in-aid for Scientific Research (C) 14570199 from the Ministry of Education, Science and Culture of Japan to Y.M. and by the Max Planck Society to R.F.

Appendix A. Supplementary data

Supplementary data associated with this article can be found, in the online version, at doi:10.1016/j.ydbio.2007.10.001.

References

Abu, E.O., et al., 1997. The localization of androgen receptors in human bone. J. Clin. Endocrinol. Metab. 82, 3493–3497.

Aszodi, A., et al., 1998. Collagen II is essential for the removal of the notochord and the formation of intervertebral discs. J. Cell Biol. 143, 1399–1412.

Aszodi, A., et al., 2003. Beta1 integrins regulate chondrocyte rotation, G1 progression, and cytokinesis. Genes Dev. 17, 2465–2479.

Chang, G.T., et al., 1997. Differentially expressed genes in androgen-dependent and -independent prostate carcinomas. Cancer Res. 57, 4075–4081.

Chang, G.T., et al., 2000. Characterization of a zinc-finger protein and its association with apoptosis in prostate cancer cells. J. Natl. Cancer Inst. 92, 1414–1421.

Chang, G.T., et al., 2002. Structure and function of GC79/TRPS1, a novel androgen-repressible apoptosis gene. Apoptosis 7, 13–21.

Fassler, R., Meyer, M., 1995. Consequences of lack of beta 1 integrin gene expression in mice. Genes Dev. 9, 1896–1908.

Fukada, T., et al., 1998. STAT3 orchestrates contradictory signals in cytokine-induced G1 to S cell-cycle transition. EMBO J. 17, 6670–6677.

Giedion, A., et al., 1973. Autosomal-dominant transmission of the tricho-rhino-phalangeal syndrome. Report of 4 unrelated families, review of 60 cases. Helv. Paediatr. Acta 28, 249–259.

Haga, S., et al., 2003. Stat3 protects against Fas-induced liver injury by redox-dependent and -independent mechanisms. J. Clin. Invest. 112, 989–998.

Hatori, M., et al., 1995. End labeling studies of fragmented DNA in the avian growth plate: evidence of apoptosis in terminally differentiated chondrocytes. J. Bone Miner. Res. 10, 1960–1968.

Itin, P.H., et al., 1996. Trichorhinophalangeal syndrome type III. Dermatology 193, 349–352.

Kaiser, F.J., et al., 2003a. The RING finger protein RNF4, a co-regulator of transcription, interacts with the TRPS1 transcription factor. J. Biol. Chem. 278, 38780–38785.

Kaiser, F.J., et al., 2003b. Nuclear interaction of the dynein light chain LC8a with the TRPS1 transcription factor suppresses the transcriptional repression activity of TRPS1. Hum. Mol. Genet. 12, 1349–1358.

Karsenty, G., Wagner, E.F., 2002. Reaching a genetic and molecular understanding of skeletal development. Dev. Cell 2, 389–406.

Kunath, M., et al., 2002. Expression of Trps1 during mouse embryonic development. Gene Expr. Patterns 2, 119–122.

Lee, C.K., et al., 2002. STAT3 is a negative regulator of granulopoiesis but is not required for G-CSF-dependent differentiation. Immunity 17, 63–72.

Levy, D.E., Lee, C.K., 2002. What does Stat3 do? J. Clin. Invest. 109, 1143–1148.

Li, L., et al., 2004. Bacterial *N*-acylhomoserine lactone-induced apoptosis in breast carcinoma cells correlated with down-modulation of STAT3. Oncogene 23, 4894–4902.

Ludecke, H.J., et al., 2001. Genotypic and phenotypic spectrum in tricho-rhino-phalangeal syndrome types I and III. Am. J. Hum. Genet. 68, 81–91.

Malik, T.H., et al., 2001. Transcriptional repression and developmental functions of the atypical vertebrate GATA protein TRPS1. EMBO J. 20, 1715–1725.

Malik, T.H., et al., 2002. Deletion of the GATA domain of TRPS1 causes an absence of facial hair and provides new insights into the bone disorder in inherited tricho-rhino-phalangeal syndromes. Mol. Cell. Biol. 22, 8592–8600.

Matsui, T., et al., 2002. STAT3 down-regulates the expression of cyclin D during liver development. J. Biol. Chem. 277, 36167–36173.

Momeni, P., et al., 2000. Mutations in a new gene, encoding a zinc-finger protein, cause tricho-rhino-phalangeal syndrome type I. Nat. Genet. 24, 71–74.

Nagai, T., et al., 1994. Another family with tricho-rhino-phalangeal syndrome type III (Sugio-Kajii syndrome). Am. J. Med. Genet. 49, 278–280.

Niikawa, N., Kamei, T., 1986. The Sugio-Kajii syndrome, proposed tricho-rhino-phalangeal syndrome type III. Am. J. Med. Genet. 24, 759–760.

Ogasawara, T., et al., 2004. Bone morphogenetic protein 2-induced osteoblast differentiation requires Smad-mediated down-regulation of Cdk6. Mol. Cell. Biol. 24, 6560–6568.

Oritani, K., 1999. Both Stat3-activation and Stat3-independent BCL2 down-regulation are important for interleukin-6-induced apoptosis of 1A9-M cells. Blood 93, 1346–1354.

Puthalakath, H., et al., 1999. The proapoptotic activity of the Bcl-2 family member Bim is regulated by interaction with the dynein motor complex. Mol. Cell 3, 287–296.

Sakai, K., et al., 2001. Stage- and tissue-specific expression of a Col2a1-Cre fusion gene in transgenic mice. Matrix Biol. 19, 761–767.

Shapiro, I.M., et al., 2005. Fate of the hypertrophic chondrocyte: microenvironmental perspectives on apoptosis and survival in the epiphyseal growth plate. Birth Defects Res., C Embryo Today 75, 330–339.

Shi, W., et al., 1996. The genomic structure and chromosomal localization of the mouse *STAT3* gene. Int. Immunol. 8, 1205–1211.

Takeda, K., et al., 1998. Stat3 activation is responsible for IL-6-dependent T cell proliferation through preventing apoptosis: generation and characterization of T cell-specific Stat3-deficient mice. J. Immunol. 161, 4652–4660.